Post-print version of the paper by Jing Deng et al. in Journal of Membrane Science, 570-571 (2019) 455-463 https://doi.org/10.1016/j.memsci.2018.10.031

Facile and Solvent-free Fabrication of PEG-based Membranes with Interpenetrating Networks for CO_2 Separation

Jing Deng,[a] **Zhongde Dai**,[a] **Jiaqi Yan**,[b] **Marius Sandru**,[c] **Eugenia Sandru**,[c] **Richard J. Spontak**[b,d] **Liyuan Deng**[a*]

[a]Department of Chemical Engineering, Norwegian University of Science & Technology, 7491 Trondheim, Norway

[b]Department of Chemical & Biomolecular Engineering, North Carolina State University, Raleigh, NC 27695, USA

[c]Department of Polymer Particles and Surface Chemistry, SINTEF Industry, 7034 Trondheim, Norway

[d]Department of Materials Science & Engineering, North Carolina State University, Raleigh, NC 27695, USA

Keywords: Polymer cross-linking; Poly(ethylene glycol); Interpenetrating networks; Aza-Michael addition; CO_2 separation membrane

Abstract

For nearly two decades, membranes derived from polyethers have served as promising candidate materials for CO_2 separation. Due to the inherent tendency of high-molecular-weight poly(ethylene oxide) (PEO) to crystallize and thus reduce its CO_2 permeability, prior studies have focused on membranes produced from low-molecular-weight poly(ethylene glycol) (PEG). In this work, a novel series of cross-linked PEG-based membranes composed of interpenetrating polymer networks has been generated through the use of amine-terminated Jeffamine and multiple acrylate-functionalized cross-linkers in a facile, solvent-free, two-stage reaction. Evidence of cross-linked interpenetrating polymer networks formed by aza-Michael addition and acrylate polymerization is confirmed by real-time Fourier-transform infrared spectroscopy. In addition, we systematically investigate the thermal stability, crystallization, mechanical properties, and water sorption of these multicomponent membranes. Corresponding CO_2 and N_2 transport properties, evaluated by single-gas permeation tests, are found to depend on both the chemical nature of the cross-linkers and the ratio of the interpenetrating networks. Moreover, free PEG dimethyl ether has been added into the optimized cross-linked matrix at different loading levels to further enhance the gas transport properties.

* To whom correspondence should be addressed (E-mail: liyuan.deng@ntnu.no).

1. Introduction

Escalating atmospheric CO_2 levels are related closely to accelerated global warming, rising sea levels and growing deterioration of typical weather patterns. To address these worrisome concerns, the development of CO_2-capture technologies designed to reduce CO_2 emission from diverse power generation sources has become increasingly urgent [1-4]. Gas-separation membranes have long been considered as a viable solution for CO_2 capture due largely to their relatively low cost, high operational simplicity and reliability, high energy efficiency, and overall environmental compatibility [2, 5-10]. For nearly 50 years, polymeric membranes have enjoyed the biggest share of the gas-separation membrane market because of the lower cost and superior processability of organic, compared to inorganic, membranes [11]. However, the performance of polymeric membranes is generally limited by a trade-off between gas permeability and selectivity [12], which means that highly permeable membranes usually possess low selectivity and *vice-versa*. Recently, several emerging polymeric materials and material classes have attracted tremendous attention for their unique ability to surpass this trade-off, or alternatively surpass the so-called Robeson upper bound, between selectivity and permeability [12]. Examples of these exceptional materials or their membranes include polymers of intrinsic microporosity (PIMs) [13-15], thermal rearrangement (TR) membranes [16-18], poly(ethylene glycol) (PEG) or poly(ethylene oxide) (PEO) membranes [19-21], and polymers endowed with specific chemical moieties to serve as carriers for facilitated gas transport [22-24]. Of particular interest here, polyether-based membranes generally possess a high intrinsic affinity towards CO_2 [10, 25]. Since high-molecular-weight PEO is semi-crystalline, however, CO_2 permeability is compromised by increased diffusive tortuosity and reduced CO_2 solubility [26]. To overcome this drawback, low-molecular-weight liquid PEG has been cross-linked [20] and/or blended with various additives to concurrently improve mechanical integrity and separation performance [25, 27].

Typical processes developed to generate gas-separation membranes are often limited to solvent-based methods, such as dip-coating, spin-coating and solution-casting [11]. The potential toxicity and large volumes of organic solvents employed in membrane production provide an ongoing impetus to explore more environment-friendly preparation approaches [28, 29]. For instance, a solvent-free method, such as a thermal reaction [21, 30] or UV-polymerization [19] of PEG, has become increasingly more attractive in membrane fabrication [20, 27]. Freeman and co-

workers [19, 31, 32] have reported that UV photopolymerization of acrylate-endcapped PEG oligomers could be used to generate amorphous membranes through which the CO_2 permeability was substantially increased. Furthermore, they have demonstrated [19] that the cross-link density of such membranes can be controllably varied by adjusting the water or PEG methyl ether acrylate (PEGMEA) level in pre-polymer solutions. Similarly, multicomponent membranes composed of PEG diacrylate (PEGDA), PEGMEA and PEG dimethyl ether (PEGDME) exhibit [20] an unprecedentedly high CO_2 permeability. A fundamental shortcoming of UV cross-linking is, however, that the free radicals generated during acrylate polymerization are sensitive to atmospheric O_2 trapped in the polymer solutions, thereby resulting in undesirable oxygen inhibition and incomplete reaction [33]. Reduction of O_2 in the reacting solution therefore requires the use of an oxygen-free glove box or a dry N_2 atmosphere. To avoid this complication, Kwisnek *et al*. [34, 35] have incorporated multifunctional thiols into acrylate-functionalized cross-linked PEG membranes to exploit the O_2 tolerance of thiol-based radicals. The resultant thiol-modified membranes possess a lower cross-link density due to a different polymerization mechanism, but enhanced gas-transport [34] and mechanical [35] properties.

In addition to free-radical polymerization, other preparation methods have also been used to form chemically cross-linked polymeric networks/membranes on the basis of diverse PEG-based monomers/oligomers. For instance, Shao *et al*. [36] have prepared cross-linked amorphous PEG membranes from the ring-opening reaction of epoxy by amine-terminated Jeffamine and report a slightly enhanced CO_2 permeability of 180 Barrer and a CO_2/N_2 selectivity of 58. They have also employed the reaction between bio-inspired dopamine and epoxy-functionalized PEG oligomer to fabricate dopamine/PEG membranes at elevated temperatures [37]. Introduction of low-molecular-weight PEGDME greatly improves gas-transport performance. Interestingly, Dai *et al*. [38] have investigated cross-linked PEG-based membranes produced from the reaction between diamine or diamine-functional ionic liquids and PEG diglycidyl ether (PEGDGE) and possessing a CO_2 permeability of ~200 Barrer after free PEGDGE is incorporated into the cross-linked network. It is noteworthy that all these reactions require a moderately high temperature ($\geq$ 80 °C) and a relatively long reaction time ($\geq$ 3 h) to complete cross-linking, and some reactions need an even more complicated preparation [36, 37], which is inconvenient for practical applications. Thus, the development of a facile, rapid and highly effective cross-linking system that employs relatively mild reaction conditions is desirable for the fabrication of PEG-based membranes.

Due to its mild reaction conditions and the absence of unwanted by-products, aza-Michael addition constitutes one of the most important reactions in organic chemistry and is crucial in the materials design of functional silicone intermediates [39], biomaterial functionalization [40] and the surface modification of membranes or nanoparticles [39, 41]. Here, we demonstrate that this reaction can likewise be applied to the preparation of novel PEG-based membranes for gas separations. Generally speaking, the aza-Michael addition refers to the addition reaction of a primary or secondary amine to an electron-deficient molecule, such as an acrylate [42-44]. Ramis and co-workers [42, 45] have proposed a dual-curing and solvent-free procedure for thermosets on the basis of aza-Michael addition (using an acrylate-amine) and acrylate photopolymerization under atmospheric conditions. The formation of tertiary amines by aza-Michael addition effectively prevents oxygen inhibition during free-radical acrylate polymerization. Moreover, the properties of the final material are tunable for diverse requirements by using different monomer species and formulation specifications. This observation is in agreement with the observations of Yang and co-workers [43, 46]. That is, by tuning the composition, monomers and reaction conditions, the network topology, swellability and other properties of the aza-Michael addition product (e.g., shape memory, environmental protection and structured surfaces) could be readily modulated.

In this work, a series of PEG-based membranes developed exclusively for CO_2 separation have been generated from aza-Michael addition and free-radical acrylate polymerization and consist of interpenetrating polymer networks. A cross-linked acrylate-amine network forms quickly at ambient temperature, while residual acrylate groups were photopolymerized under UV radiation. The cross-link density can be controlled by the choice of cross-linker at different compositions, and addition of a PEG-based oligomer serves to induce network swelling and improve gas transport. The chemical structure, thermal properties and single-gas permeation of the resultant membranes are investigated here by various characterization techniques.

2. Experimental

2.1 Materials

Pentaerythritol triacrylate (PEG3A), pentaerythritol tetraacrylate (PEG4A), 1-hydroxylcyclohexyl phenyl ketone (HCPK), Jeffamine and PEGDME were all purchased from Sigma Aldrich. Dipentaerythritol hexaacrylate (PEG5A) was obtained from Abcr. All chemicals

were used as-received without further purification. The chemical structures of these monomer species are displayed in **Figure 1**.

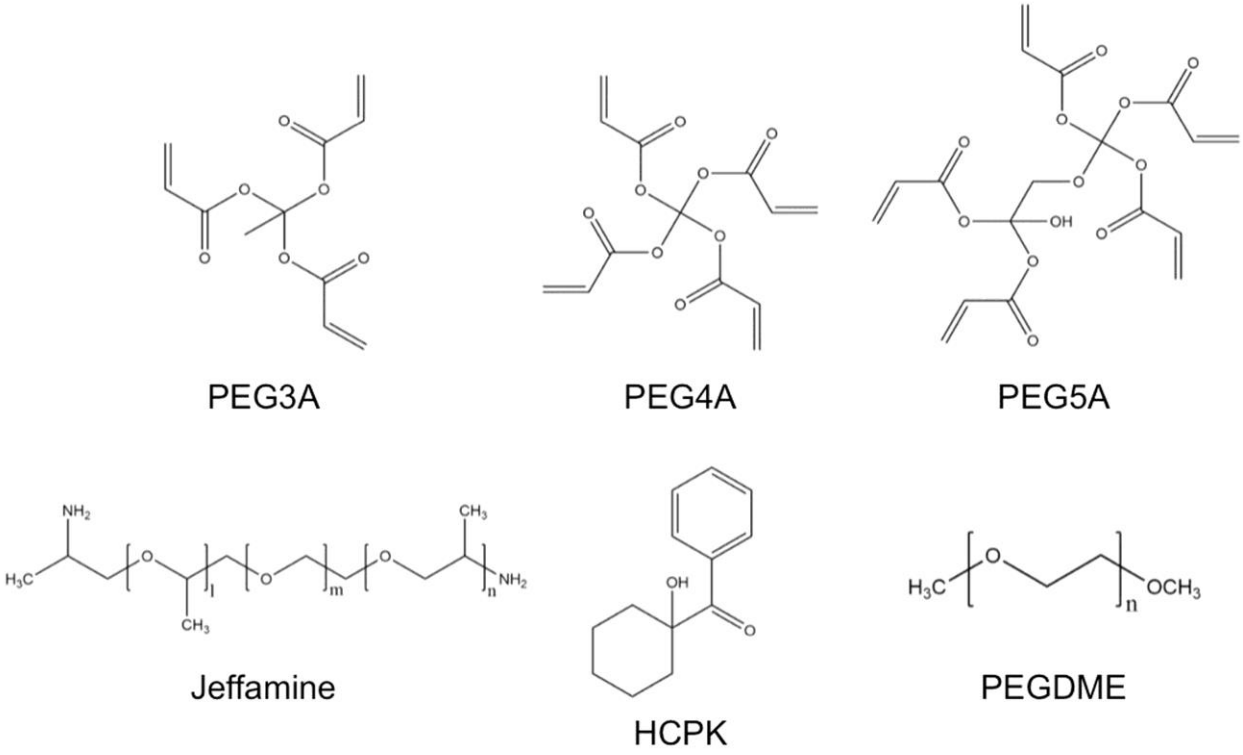

Figure 1. Chemical structures of the monomers and cross-linkers employed in this study: PEG3A, PEG4A, PEG5A, Jeffamine, HCPK and PEGDME.

2.2 Membrane preparation

Membranes were fabricated by a two-stage cross-linking reaction similar to that described elsewhere [19, 42]. A brief description of the reaction scheme, illustrated in **Figure 2**, is presented here. Multiple acrylate-functionalized cross-linkers, free PEGDME and 0.01-0.1 wt% HCPK were combined in a glass vial for several minutes to ensure homogeneous mixing. The mass ratio of PEGDME (w_{PEGDME}) was calculated from

$$W_{PEGDME} = \frac{m_{PEGDME}}{m_{Cross-linker}} \times 100\% \qquad (1)$$

A known amount of Jeffamine was added to the mixture under vigorous stirring to promote complete reaction. The mole ratio of cross-linkers and Jeffamine was calculated on the basis of acrylate groups to amine bonds. The mixture was then transferred to a vacuum oven to remove the likelihood of bubbles. Afterwards, the solution was sandwiched between two quartz plates

separated by spacers to control the membrane thickness. The solution was photopolymerized under a UV lamp (UVLS-28, Ultra-Violet Products Ltd.) with a wavelength of 365 nm for 2 h. The resultant membranes were evaluated by various characterization methodologies and permeation tests. In this work, all membranes are systematically designated as "Cross-linker-Jeffamine-X-X" according to the constituent species and the ratio of acrylate-containing cross-linker to amine-terminated monomer. For example, the PEG3A-J-6-1 membrane consists of PEG3A and Jeffamine with 6 PEG3A acrylate groups per 1 Jeffamine N-H bond.

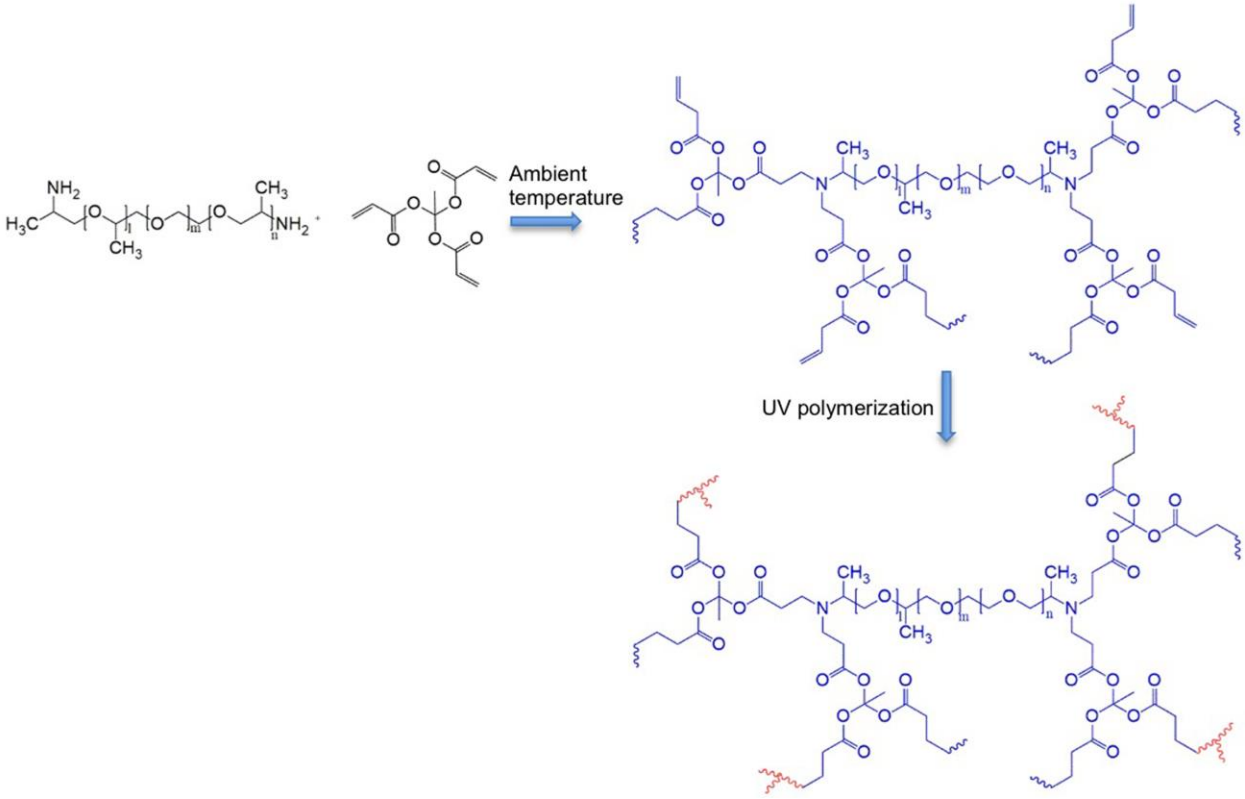

Figure 2. Schematic illustration of a portion of the PEG3A-Jeffamine interpenetrating network.

2.3 Membrane characterization

A Thermo Nicolet Nexus Fourier-transform infrared (FTIR) spectrometer with an attenuated total reflectance (ATR) cell equipped with a diamond crystal was used to collect chemical spectra from all the membranes in this study. To monitor the real-time reaction between cross-linker and Jeffamine, the Marco-Real protocol was employed: a drop of mixture solution containing cross-linker and Jeffamine was placed on the diamond crystal, heated to 30 °C and covered by a glass Petri dish. Spectra were recorded every 1.5 min over the course of 1 h under isothermal conditions.

The thermal stability of the membranes was interrogated by thermogravimetric analysis (TGA) performed on a Thermal Scientific Q500 instrument. Approximately 10-20 mg samples were heated in a ceramic crucible from ambient temperature to 700 °C at a constant heating rate of 10 °C/min under N_2 to prevent thermo-oxidative degradation of the membranes. The bulk mechanical properties of the membranes were investigated by performing quasistatic uniaxial tensile tests on an Instron Universal Machine 5943. Samples measuring ~500 µm thick were cut into strips measuring 4.0 cm x 1.0 cm with a CO_2 laser on a Universal Laser VLS3.50 system. The samples were subjected to a crosshead speed of 10 mm/min. Each membrane thickness was discerned as the average of 5 measurements. Water-uptake tests were conducted to evaluate the hydrophilicity of the membranes, as well as their swellability. Membrane specimens were placed in a closed container saturated with water vapor at ambient temperature. The subsequent increase in weight was measured until it stabilized. The water uptake (W_{H2O}) of membranes was calculated by

$$W_{H_2O} = \frac{W_f - W_0}{W_0} \times 100\% \qquad (2)$$

where W_f is the final (stabilized) specimen weight and W_0 represents the initial weight.

In this work, the gas permeability (P) of either CO_2 or N_2 through the membranes was measured by the constant-volume variable-pressure method according to

$$\mathrm{P} = \left[\left(\frac{\mathrm{dp_d}}{\mathrm{dt}}\right)_{\mathrm{t}\to\infty} - \left(\frac{\mathrm{dp_d}}{\mathrm{dt}}\right)_{\mathrm{t}\to\mathrm{leak}}\right] \cdot \frac{\mathrm{V_d}}{\mathrm{A}\cdot\mathrm{R}\cdot\mathrm{T}} \cdot \frac{\mathrm{l}}{(\mathrm{p_u} - \mathrm{p_d})} \qquad (3)$$

where p_d and p_u identify the downstream and upstream gas pressures, respectively, and t is time. Here, V_d is the downstream volume, A corresponds to the effective permeation area of membrane, R is the universal gas constant, T denotes absolute temperature, and l is the membrane thickness. The leakage rate of the gas permeation setup $(^{dp_d}/_{dt})_{t\to leak}$ was measured from the increase in pressure relative to vacuum over time. Membrane thicknesses were measured by a Digitix II thickness gauge. Average thicknesses were averaged from more than 10 measurements for each membrane. All gas permeation experiments were performed using an upstream pressure of 2 bar (absolute) at ambient temperature. For each membrane, the reported permeabilities were the average of measurements acquired from at least two specimens. The ideal CO_2/N_2 selectivity was

calculated from the ratio of gas permeabilities in accord with

$$\alpha_{ij} = \frac{P_i}{P_j} \quad (4)$$

Furthermore, the diffusion coefficient (D) was evaluated by the time-lag method from the single-gas permeation tests:

$$D = \frac{l^2}{6 \cdot \theta} \quad (5)$$

where θ corresponds to the time from the start of the measurement to the time when steady state is achieved in permeation tests. Accompanying solubility (S) values were calculated from the permeability and diffusivity assuming applicability of the solution-diffusion mechanism in the Fickian regime so that

$$S = \frac{P}{D} \quad (6)$$

3. Results and Discussion

3.1 Cross-linking mechanism

To confirm the aza-Michael addition between acrylate and amine groups, we have performed real-time FTIR-ATR analysis of mixtures composed of Jeffamine and PEG3A. Since the amine content in Jeffamine is relatively low, the peak corresponding to the -NH_2 group (at 3100-3500 cm^{-1}) is imperceptible, in which case changes in the acrylate group are used to follow the reaction. The intensity of the peaks corresponding to the -C=C- stretching band (at 1637 cm^{-1}) and the =C-H band (at 1408 and 808 cm^{-1}) are observed to decrease significantly with increasing time in **Figure 3**, thereby confirming that the acrylate groups are consumed. Considering that the amine is the only functional group that is capable of reacting with the acrylate and that acrylate cannot self-react rapidly in the absence of catalyst in this system, this result confirms the reaction between Jeffamine and PEG3A. In addition, the peak intensities related to the C=C and =C-H bonds decrease sharply at early measurement times but become less time-dependent as the reaction progresses, in agreement of the typical kinetics characteristic of a step-growth mechanism such as aza-Michael polymerization [47]. The PEG3A is first expected to react rapidly with Jeffamine to

form star-like oligomers, which subsequently react with each other and grow to build a cross-linked network. As mentioned earlier, this reaction proceeds much more slowly during real-time measurement (without constant stirring) when compared to the reaction under film preparation conditions.

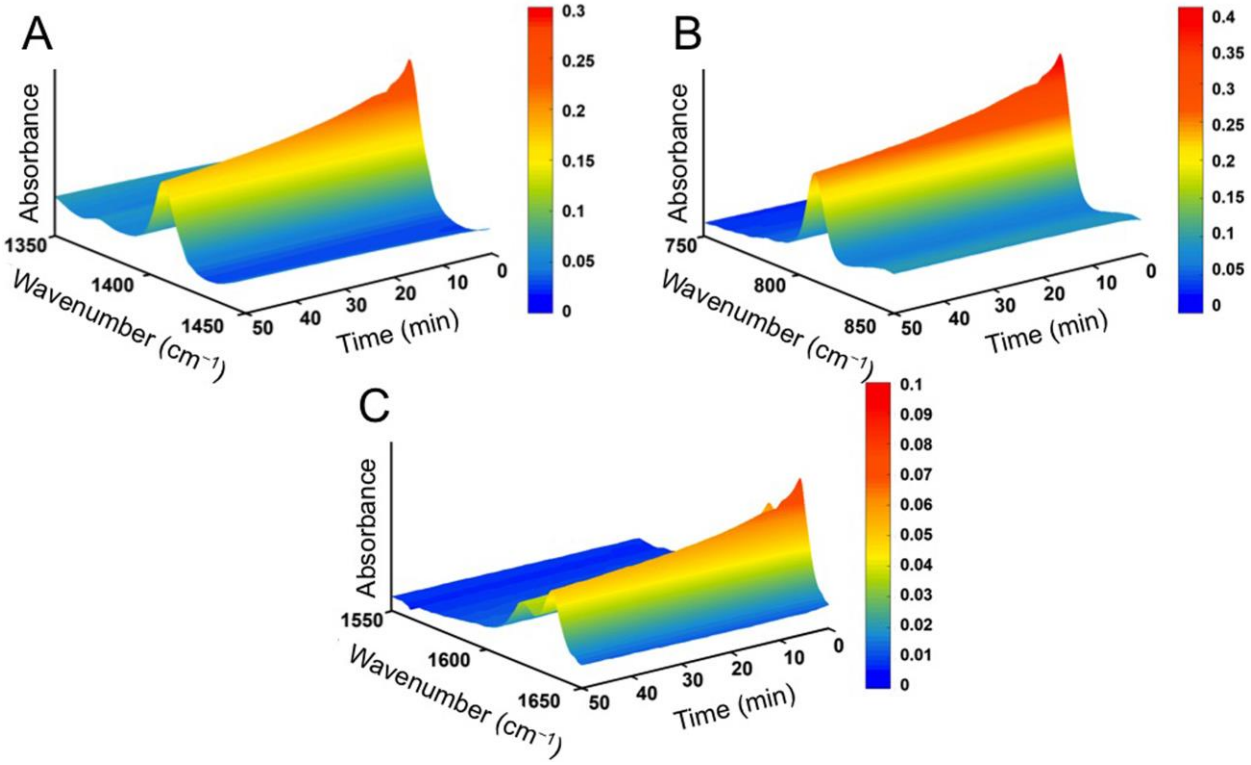

Figure 3. Real-time FTIR spectra of a PEG3A/Jeffamine reaction mixture with 1:1 w/w ratio collected over three different regions (in cm^{-1}): (A) 750-850, (B) 1350-1450 and (C) 1550-1650.

The effect of aza-Michael addition is also apparent from the spectra of the final membranes, as evidenced in **Figure 4**. A signal corresponding to residual –C=C- bonds remains in FT-IR spectra acquired from PEG3A or PEG3A-J membranes with sufficient irradiation (2h instead of the regular 90 s – 3 min [31]), indicating incomplete conversion of acrylate. The peak intensity of acrylate in these final membranes decreases upon addition of Jeffamine. These observations could result from several considerations. First, the cross-linkers used in this works are multifunctional, in which case considerable steric hindrance might yield isolated C=C groups during the cross-linking reaction. In addition, oxygen inhibition might also contribute to the low conversion of acrylate during homo-polymerization [33]. Addition of Jeffamine with longer chains is anticipated

to increase the distance between cross-linking sites and reduce steric hindrance. Moreover, the aza-Michael addition overcomes oxygen inhibition of free-radical acrylate polymerization to achieve higher acrylate conversion. Lastly, as the concentration of Jeffamine is increased, typical peaks associated with the ether and methyl groups ((at 1102 and 2867 cm^{-1}, respectively) corresponding to Jeffamine become more conspicuous in the FTIR spectra, suggesting an increase in the fraction of ethylene glycol units, which is further expected to benefit CO_2 transport and improve CO_2 separation performance.

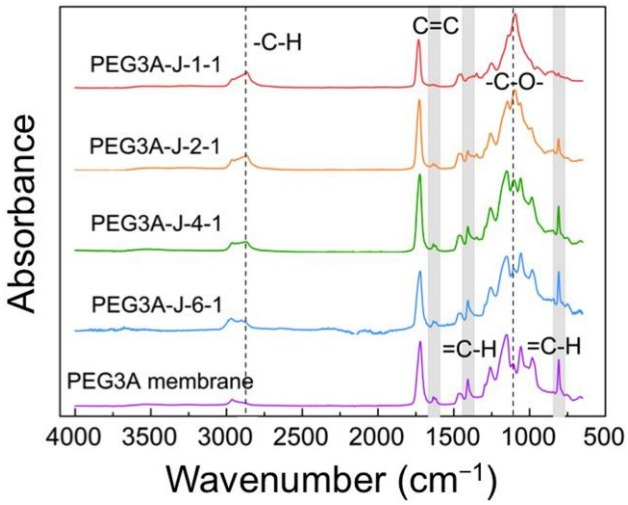

Figure 4. FTIR spectra of PEG3A and four PEG3A-J membranes varying in Jeffamine content (labeled and color-coded). Specific spectral peaks discussed in the text are highlighted.

3.2 Bulk properties

The thermal stability of PEG3A-J and PEG3A membranes has been investigated by TGA (*cf.* **Figure 5**). These results reveal that all the membranes investigated here exhibit single-stage thermal decomposition, with the decomposition temperature varying between 300 and 400 °C, depending on the formulation details. An increase in amine content is, however, accompanied by a progressive reduction in the thermal stability of the PEG3A-J membranes. This behavior is attributed to the intrinsic properties of the C-C and C-N bonds, since C-N bonds are known to be less thermally stable than C-C bonds [42]. Although these results demonstrate that the thermal stability of acrylate/amine-based membranes is compromised upon addition of amine, all the membranes possess sufficient thermal stability for CO_2 separation membranes intended for use in

post-combustion and natural-gas sweetening, which are normally operated at temperatures below 80 °C. Since these membranes must likewise possess sufficient mechanical resilience, the mechanical properties of PEG3A-J and PEG3A membranes have been evaluated by quasistatic uniaxial tensile testing (according to ASTM D882-1223 and displayed in **Figure 6A**). All the membranes undergo catastrophic failure over a relatively narrow strain range (< 13%) with only PEG3A-J-1-1 displaying evidence of elastomeric behavior. From these strain-stress curves, the PEG3A-J membranes are found to be less brittle compared to the neat PEG3A membranes, and an increase in Jeffamine content promotes an increase in the maximum strain and a corresponding reduction in tensile strength. The tensile modulus, which quantifies the stiffness of a solid material [48] and is calculated from either the initial slope of the stress-strain curve or the stress measured at 2% strain, is observed in **Figure 6B** to decrease with increasing Jeffamine fraction. Tensile strength values, identified as the maximum stresses observed in **Figure 6A** and included in **Figure 6B**, indicates a slight maximum, but does not change appreciably, with increasing Jeffamine content. Also included in the inset of **Figure 6B** are the elongation-at-break (discerned at the tensile strength) and the relative fracture toughness (measured from the area under each stress-strain curve and normalized with respect to the value determined for PEG3A). We therefore conclude that the PEG3A-J membranes become softer (lower tensile modulus) and weaker (lower tensile strength) but more stretchable (larger maximum strain) and tougher (larger fracture toughness) as the N-H/acrylate ratio is systematically increased. These changes are believed to be due to the longer chains afforded by the addition of Jeffamine.

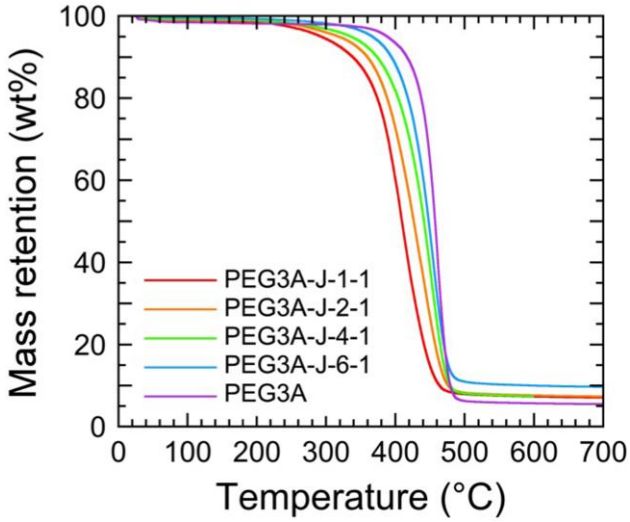

Figure 5. Mass retention measured by TGA and presented as a function of temperature for PEG3A and four

PEG3A-J membranes varying in Jeffamine content (color-coded).

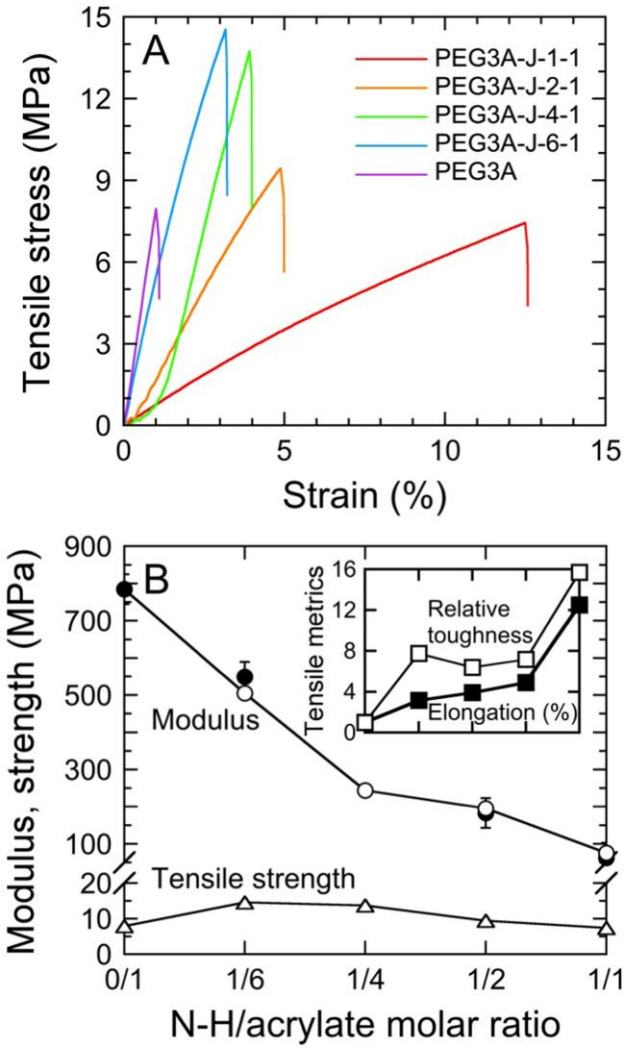

Figure 6. (A) Quasistatic uniaxial tensile tests measured from PEG3A-J and four PEG3A membranes varying in Jeffamine content (color-coded). (B) Moduli measured from the initial slope up to 1% strain (●) or the stress value at 2% strain (○), as well as the tensile strength (△) determined from the maximum stress, of the data displayed in (A) as functions of the N-H/acrylate molar ratio. Included in the inset are the maximum strain (or elongation, in %) and relative fracture toughness (labeled). The solid lines in (B) serve to connect the data.

Gas-separation performance can be significantly improved by the presence of water vapor for hydrophilic membranes such as polyvinylamine [49, 50] , poly(acrylic acid) [51], poly(vinyl alcohol) [52, 53], and ionic liquid-containing membranes [54-56]. Several factors could be responsible for such improvement: enhanced polymer chain mobility, highly permeable water-swollen regions or facilitated transport arising from specific functional moieties. For comparison,

we examine the effect of water sorption on the present membrane materials. **Figure 7** displays water uptake results measured from the PEG3A-J membranes at ambient temperature and immediately reveals that these membranes with different interpenetrating networks exhibit different hydrophilicity levels. The extremely low water uptake (< 2 wt%) of the parent PEG3A membrane is a direct consequence of its high cross-link density. Water uptake increases slightly upon addition of Jeffamine, ultimately resulting in 48.5 wt% for PEG3A-J-1-1, which does not contain interpenetrate networks connected by C-C and C-N bonds. Since C-C bonds are less hydrophilic than C-N bonds, the existence of more C-C bonds in the PEG3A-J-1-2 membrane reduces its bulk hydrophilicity, as reflected by its lower water uptake of 9.2 wt% in **Figure 7**.

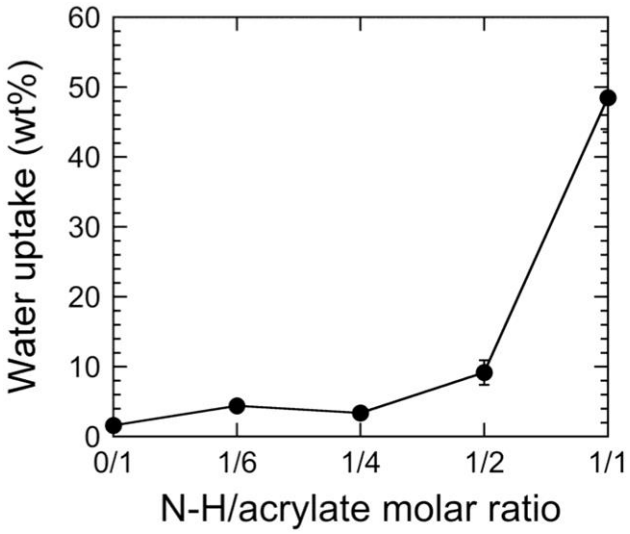

Figure 7. Water uptake presented as a function of N-H/acrylate molar ratio for PEG3A and four PEG3A-J membranes varying in Jeffamine content. The solid lines serves to connect the data.

3.3 Permeability considerations

To ascertain the influence of cross-linker functionality on the gas-separation performance, cross-linked PEG membranes have been prepared from three cross-linking agents possessing different functional groups (PEG3A, PEG4A and PEG5A) at a constant N-H:acrylate ratio of 1:4. The single-gas transport properties of these membranes have been tested at ambient temperature with a feed pressure of 2.0 bar and a vacuum level of 1 mbar on the permeate side. The CO_2 and N_2 permeabilities of these membranes, as well as the corresponding CO_2/N_2 ideal selectivities, are presented in **Table 1**. Theoretically, an increase in the fraction of acrylate groups contained in the cross-linkers is expected to generate membranes with a higher cross-link density and lower gas

permeability, which agrees with the N_2 permeability of these membranes. The CO_2 permeability of PEG5A-J-4-1 appears to increase slightly relative to PEG4A-J-4-1, but this difference lies within the range of experimental uncertainty. Taken together, these results suggest that gas permeability decreases (or at least does not change significantly) as the number of acrylate groups in the cross-linkers is increased. Due largely to the dependence of N_2 permeability on cross-linker functionality, the CO_2/N_2 ideal selectivity increases with increasing acrylate content, a result of higher cross-link density. Because of such high cross-link density, all membranes display relatively low gas permeability and moderate CO_2/N_2 selectivity. To improve gas-transport properties, we have chosen the PEG3A cross-linker for further study in this work.

Table 1. The effect of different cross-linkers on gas-separation performance.

Membrane	P_{CO2} (Barrer)	P_{N2} (Barrer)	CO_2/N_2 ideal selectivity
PEG3A-J-4-1	3.73 ± 0.50	0.10 ± 0.03	36.5 ± 6.0
PEG4A -J-4-1	1.94 ± 0.31	0.05 ± 0.01	38.7 ± 9.2
PEG5A-J-4-1	2.68 ± 0.47	0.04 ± 0.02	46.7 ± 8.2

The effect of dual cross-linked networks on the gas-separation performance of PEG3A-J membranes is interrogated by systematically varying the ratio between amine bonds and acrylate group. In **Figure 8a**, CO_2 permeability and CO_2/N_2 ideal selectivity values are provided as functions of the N-H/acrylate molar ratio. While the CO_2 permeability of cross-linked PEG3A is low (≈1.56 Barrer) and the corresponding CO_2/N_2 selectivity is about 29, introduction of the cross-linked N-H/amine network enhances CO_2 permeability and becomes more effective with increasing N-H/acrylate ratio. Since N_2 permeability likewise increases with increasing N-H/acrylate ratio, the CO_2/N_2 ideal selectivity is only marginally improved to just under 40 and then remains relatively constant. Since the CO_2-philic groups in both PGE3A and Jeffamine are ether groups, these two materials are reasonably expected to possess similar CO_2/N_2 selectivities. The reason for CO_2 permeability enhancement in the PEG3A-J membranes is related to either the diffusivity or solubility of CO_2 in the membranes. These values, calculated from Eqs. (5) and (6), respectively, are included in **Figure 8b**. The CO_2 diffusivity displays a monotonic increase as the N-H/acrylate ratio is increased, indicating that the acrylate/amine cross-linked network becomes increasingly less dense, which is responsible for promoting a 5x increase in CO_2 diffusivity relative

to that in the neat acrylate cross-linked membrane and for following the same trend as membrane stiffness (according to the tensile modulus in **Figure 6**). As mentioned earlier, Jeffamine possesses a longer chain than PEG3A, which extends the distance between cross-link sites and generates a more flexible network, resulting in a higher CO_2 diffusivity. On the other hand, CO_2 solubility initially displays a slight reduction (very close to experimental uncertainty) from 0.031 to 0.027 cm^3(STP)/(cm^3-cm Hg) as the N-H/acrylate ratio is increased from 0:1 to 1:2. A decrease in CO_2 solubility over this range could be due to the lower CO_2 affinity for propylene oxide relative to ethylene oxide [30]. Further increasing the N-H/acrylate ratio to 1:1 promotes a considerably higher CO_2 solubility of 0.073 cm^3(STP)/(cm^3-cm Hg) in the PEG3A-J-1-1 membrane. This sudden increase is attributed to the positive effect of the presence of additional C-N bonds.

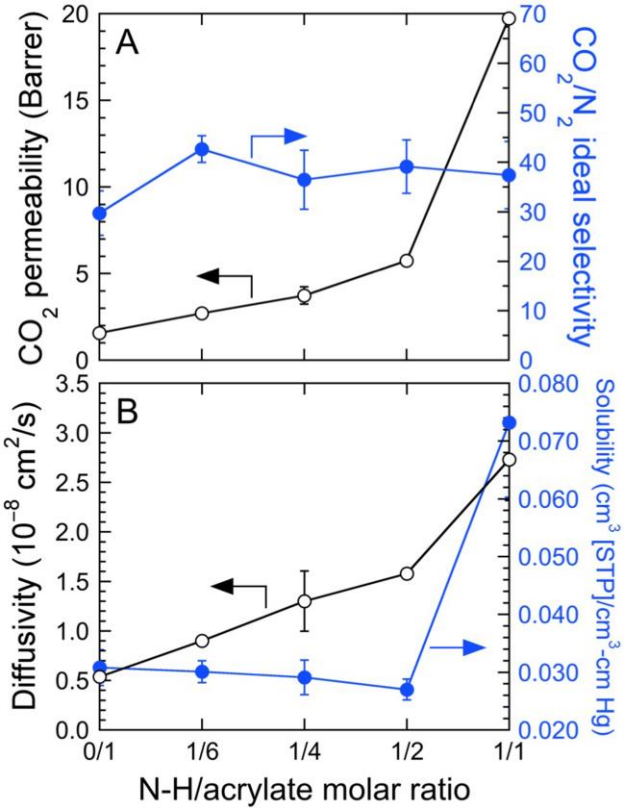

Figure 8. (A) CO_2 permeability and CO_2/N_2 ideal selectivity as functions of the N-H/acrylate ratio (color-coded). (B) Corresponding CO_2 diffusivity and CO_2 solubility values of the PEG3A and PEG3A-J membranes (similarly color-coded). The solid lines serve to connect the data.

A low-molecular-weight PEG additive (PEGDME) has been incorporated into the PEG3A-J membranes to further improve gas-separation performance. The PEG3A-J-4-1 membrane is selected for this analysis due to its promising mechanical stability. Both CO_2 permeability and

CO_2/N_2 ideal selectivity are shown as functions of PEGDME content in **Figure 9a**. As expected, the CO_2 permeability systematically increases with increasing PEGDME loading level, from 3.7 Barrer in the PEGDME-free membrane to 196.4 Barrer in the membrane with 100% PEGDME incorporation. The CO_2/N_2 ideal selectivity increases with increasing PEGDME content up to ≈50 wt% PEGDME and then remains constant. Corresponding values of the CO_2 diffusivity and solubility in PEG3A-J-PEGDME membranes are also provided in **Figure 9b**. By increasing the PEGDME content, the CO_2 diffusivity increases monotonically, while the CO_2 solubility fluctuates most likely within the range of experimental uncertainty. The similarity of CO_2 solubilities measured for membranes with and without added PEGDME is explained by the comparable affinity of PEG-based material for CO_2. Therefore, the increase in CO_2 permeability due to the addition of PEGDME is mainly attributed to the increase in CO_2 diffusivity, whereas the CO_2/N_2 ideal selectivity relates to the CO_2 solubility. The increase in CO_2 diffusivity with PEGDME level could be explained by two effects. Addition of low-molecular-weight CO_2-philic species in the membrane is expected to form fast diffusion zones so that CO_2 molecules will migrate more readily through these regions [38, 57]. Moreover, the presence of PEGDME during membrane formation can alternatively lead to larger distances between cross-link sites, resulting in larger unobstructed gas-transport pathways. The overall performance of the membranes prepared and examined in this study, as well as the state-of-the-art PEG-based membranes, are compared in the Robeson trade-off plot provided in **Figure 10**. Detailed data from selected literature sources are likewise listed in **Table 2**. As is evident from these comparisons, the gas-separation performance of PEG3A-J-PEGDME membranes approaches the upper bound and becomes comparable to other recently reported PEG-based membranes prepared by common solvent evaporation methods.

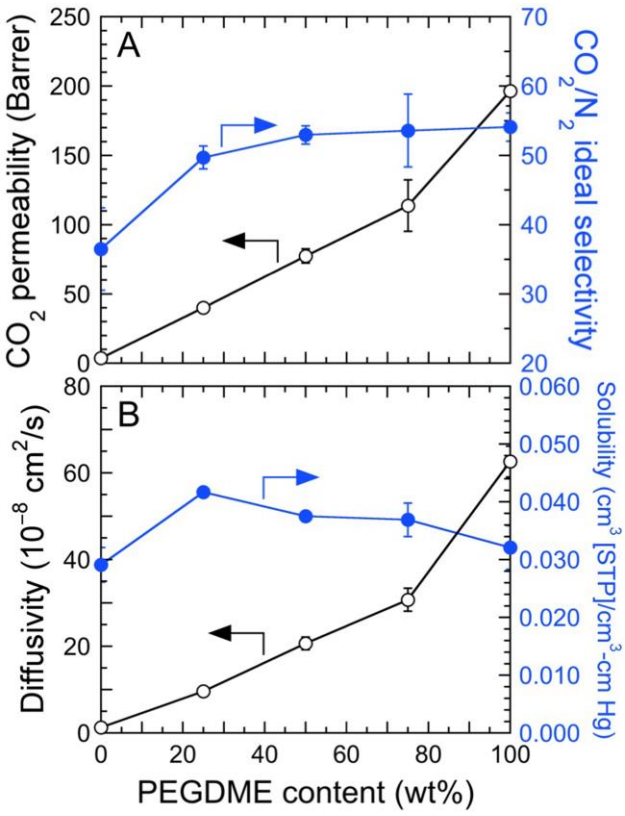

Figure 9. (A) CO_2 permeability and CO_2/N_2 ideal selectivity as functions of PEGDME content in the PEG3A-J-4-1 membrane (color-coded). (B) Corresponding CO_2 diffusivity and CO_2 solubility values of the same PEGDME-containing membranes (similarly color-coded). The solid lines serve to connect the data.

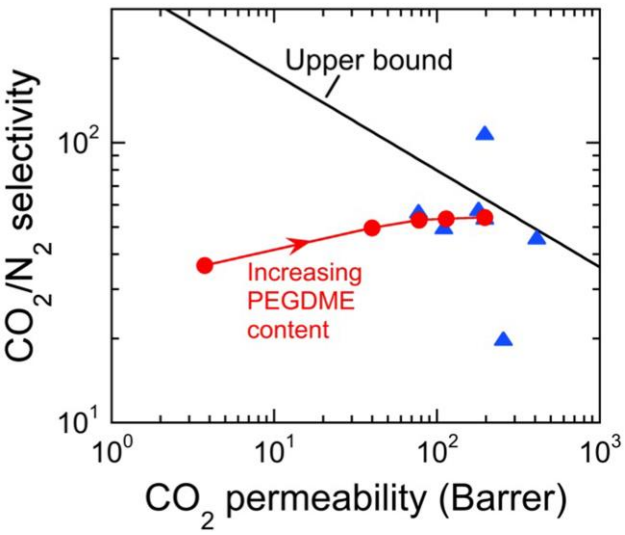

Figure 10. Values of CO_2 permeability and CO_2/N_2 selectivity evaluated here from the PEG3A-J-4-1 membrane at several PEGDME loading levels (●). Comparable data gleaned from the literature and listed in **Table 2** are included for comparison (▲). The solid line through the data serves as a guide for the eye, whereas the line identifying the

Robeson upper bound is labeled.

Table 2. CO_2/N_2 separation performance of cross-linked PEG-based membranes measured in this work and reported elsewhere.

Membrane	P_{CO2} (Barrer)	CO_2/N_2 selectivity	Reference
XLPEGDA[a]	110	50	[19]
Poly(TEGMVE:VEEM)[b]	410	46	[58]
PEGDMA/SiGMA copolymers	255	20	[59]
Thiol-containing PEG	77	57	[34]
PEG cross-linked with A-amine (80% free PEGDME)	196	108	[38]
PEGDGE cross-linked with Jeffamine	180	58	[36]
PEG-Jeffamine (100% free PEGDME)	196	54	This work

[a] Cross-linked PEGDA (molecular weight: 743 g/mol)
[b] TEGMVE: [2-(2-(2-methoxyethoxy)ethoxy)ethyl vinyl ether), VEEM: 2-(2-vinyloxyethoxy)ethyl methacrylate

4. Conclusions

In this work a series of PEG-based materials with interpenetrating polymeric networks has been synthesized and fabricated into membranes for CO_2 separation. The preparation procedure is based on a facile and solvent-free two-stage cross-linking process based on aza-Michael addition and acrylate photopolymerization. Results from FTIR spectroscopy confirm the cross-linking mechanisms and indicate the existence of dual cross-link networks. The thermal stability of all the membranes indicate that these membranes become less stable with increasing amine content but are nonetheless suitable for CO_2 separation processes. Addition of Jeffamine softens and toughens the membranes by introducing longer polymer chains and improving the flexibility of the cross-linked network. An amine-induced increase in water uptake confirms that the hydrophilic properties of the membranes are improved by incorporation of Jeffamine. Although not investigated here, this dependence might benefit CO_2 separation under humid conditions. Three multi-acrylate functionalized cross-linkers have been reacted with Jeffamine. Single-gas permeation results confirm that cross-linkers with fewer acrylate groups induce lower cross-link densities and better gas-transport properties. Cross-linked PEG membranes possessing a high N-H/acrylate ratio display a high CO_2 permeability. Incorporation of free PEGDME in the optimized membrane yields a significantly enhanced CO_2 permeability that is largely attributed to an increase in CO_2 diffusivity without sacrificing the CO_2/N_2 ideal selectivity. Overall, this two-stage cross-linking method constitutes a straightforward and effective solvent-free route to prepare self-standing cross-linked PEG-based membranes with excellent CO_2 separation performance. In addition, the results reported herein have established that the molecular, transport and bulk properties of these membranes are all highly tunable, which affords practical advantages for feasible membrane preparation under environmentally-benign conditions.

Acknowledgments

This work was supported at the Norwegian University of Science & Technology and SINTEF Industry by the Research Council of Norway through the CLIMIT program (POLYMEM project, No. 254791) and at North Carolina State University by the Nonwovens Institute.

References

[1] H. Yang, Z. Xu, M. Fan, R. Gupta, R.B. Slimane, A.E. Bland, I. Wright, Progress in carbon dioxide separation and capture: A review, J. Environ. Sci., 20 (2008) 14-27.
[2] D.M. D'Alessandro, B. Smit, J.R. Long, Carbon dioxide capture: Prospects for new materials, Angew. Chem. Int. Ed., 49 (2010) 6058-6082.
[3] S. Zeng, X. Zhang, L. Bai, X. Zhang, H. Wang, J. Wang, D. Bao, M. Li, X. Liu, S. Zhang, Ionic-liquid-based CO_2 capture systems: Structure, interaction and process, Chem. Rev., 117 (2017) 9625-9673.
[4] C.E. Powell, G.G. Qiao, Polymeric CO_2/N_2 gas separation membranes for the capture of carbon dioxide from power plant flue gases, J. Membr. Sci., 279 (2006) 1-49.
[5] M. Galizia, W.S. Chi, Z.P. Smith, T.C. Merkel, R.W. Baker, B.D. Freeman, 50th anniversary perspective: polymers and mixed matrix membranes for gas and vapor separation: a review and prospective opportunities, Macromolecules, 50 (2017) 7809-7843.
[6] S. Kim, Y.M. Lee, High performance polymer membranes for CO_2 separation, Curr. Opin. Chem. Eng., 2 (2013) 238-244.
[7] X. Zhang, B. Singh, X. He, T. Gundersen, L. Deng, S. Zhang, Post-combustion carbon capture technologies: energetic analysis and life cycle assessment, Int. J. Greenh. Gas Con., 27 (2014) 289-298.
[8] M.-B. Hägg, L. Deng, Membranes in gas separation, in: Handbook of membrane separations: chemical, pharmaceutical, food, and biotechnological applications, CRC Press, Boca Raton, FL, 2015, pp. 143-180.
[9] Z. Dai, R.D. Noble, D.L. Gin, X. Zhang, L. Deng, Combination of ionic liquids with membrane technology: A new approach for CO_2 separation, J. Membr. Sci., 497 (2016) 1-20.
[10] S. Wang, X. Li, H. Wu, Z. Tian, Q. Xin, G. He, D. Peng, S. Chen, Y. Yin, Z. Jiang, Advances in high permeability polymer-based membrane materials for CO_2 separations, Energy Environ. Sci., 9 (2016) 1863-1890.
[11] Z. Dai, L. Ansaloni, L. Deng, Recent advances in multi-layer composite polymeric membranes for CO_2 separation: a review, Green Energy Environ., 1 (2016) 102-128.
[12] L.M. Robeson, The upper bound revisited, J. Membr. Sci., 320 (2008) 390-400.
[13] M. Carta, R. Malpass-Evans, M. Croad, Y. Rogan, J.C. Jansen, P. Bernardo, F. Bazzarelli, N.B. McKeown, An efficient polymer molecular sieve for membrane gas separations, Science, 339 (2013) 303-307.
[14] N.B. McKeown, P.M. Budd, K.J. Msayib, B.S. Ghanem, H.J. Kingston, C.E. Tattershall, S. Makhseed, K.J. Reynolds, D. Fritsch, Polymers of intrinsic microporosity (PIMs): bridging the void between microporous and polymeric materials, Chem. Eur. J., 11 (2005) 2610-2620.
[15] P.M. Budd, N.B. McKeown, B.S. Ghanem, K.J. Msayib, D. Fritsch, L. Starannikova, N. Belov, O. Sanfirova, Y. Yampolskii, V. Shantarovich, Gas permeation parameters and other physicochemical properties of a polymer of intrinsic microporosity: Polybenzodioxane PIM-1, J. Membr. Sci., 325 (2008) 851-860.
[16] H.B. Park, C.H. Jung, Y.M. Lee, A.J. Hill, S.J. Pas, S.T. Mudie, E. Van Wagner, B.D. Freeman, D.J. Cookson, Polymers with cavities tuned for fast selective transport of small molecules and ions, Science, 318 (2007) 254-258.
[17] H.B. Park, S.H. Han, C.H. Jung, Y.M. Lee, A.J. Hill, Thermally rearranged (TR) polymer membranes for CO_2 separation, J. Membr. Sci., 359 (2010) 11-24.

[18] S.H. Han, N. Misdan, S. Kim, C.M. Doherty, A.J. Hill, Y.M. Lee, Thermally rearranged (TR) polybenzoxazole: effects of diverse Imidization routes on physical properties and gas transport behaviors, Macromolecules, 43 (2010) 7657-7667.
[19] H. Lin, T. Kai, B.D. Freeman, S. Kalakkunnath, D.S. Kalika, The effect of cross-linking on gas permeability in cross-linked poly(ethylene glycol diacrylate), Macromolecules, 38 (2005) 8381-8393.
[20] X. Jiang, S. Li, L. Shao, Pushing CO_2-philic membrane performance to the limit by designing semi-interpenetrating networks (SIPN) for sustainable CO_2 separations, Energy Environ. Sci., 10 (2017) 1339-1344.
[21] N.P. Patel, A.C. Miller, R.J. Spontak, Highly CO_2- permeable and selective polymer nanocomposite membranes, Adv. Mater., 15 (2003) 729-733.
[22] L. Deng, T.-J. Kim, M.-B. Hägg, Facilitated transport of CO_2 in novel PVAm/PVA blend membrane, J. Membr. Sci., 340 (2009) 154-163.
[23] J. Liao, Z. Wang, C. Gao, S. Li, Z. Qiao, M. Wang, S. Zhao, X. Xie, J. Wang, S. Wang, Fabrication of high-performance facilitated transport membranes for CO_2 separation, Chem. Sci., 5 (2014) 2843-2849.
[24] J. Zou, W.S.W. Ho, CO_2-selective polymeric membranes containing amines in crosslinked poly(vinyl alcohol), J. Membr. Sci., 286 (2006) 310-321.
[25] S.L. Liu, L. Shao, M.L. Chua, C.H. Lau, H. Wang, S. Quan, Recent progress in the design of advanced PEO-containing membranes for CO_2 removal, Prog. Polym. Sci., 38 (2013) 1089-1120.
[26] H. Lin, B.D. Freeman, Gas solubility, diffusivity and permeability in poly (ethylene oxide), J. Membr. Sci., 239 (2004) 105-117.
[27] S. Wang, X. Li, H. Wu, Z. Tian, Q. Xin, G. He, D. Peng, S. Chen, Y. Yin, Z. Jiang, Advances in high permeability polymer-based membrane materials for CO_2 separations, Energy & Environmental Science, 9 (2016) 1863-1890.
[28] G. Szekely, M.F. Jimenez-Solomon, P. Marchetti, J.F. Kim, A.G. Livingston, Sustainability assessment of organic solvent nanofiltration: from fabrication to application, Green Chem., 16 (2014) 4440-4473.
[29] A. Figoli, T. Marino, S. Simone, E. Di Nicolò, X.M. Li, T. He, S. Tornaghi, E. Drioli, Towards non-toxic solvents for membrane preparation: a review, Green Chem., 16 (2014) 4034-4059.
[30] N.P. Patel, A.C. Miller, R.J. Spontak, Highly CO_2- permeable and- selective membranes derived from crosslinked poly (ethylene glycol) and its nanocomposites, Adv. Funct. Mater., 14 (2004) 699-707.
[31] H. Lin, B.D. Freeman, Gas and vapor solubility in cross-linked poly(ethylene glycol diacrylate), Macromolecules, 38 (2005) 8394-8407.
[32] H. Lin, E.V. Wagner, J.S. Swinnea, B.D. Freeman, S.J. Pas, A.J. Hill, S. Kalakkunnath, D.S. Kalika, Transport and structural characteristics of crosslinked poly(ethylene oxide) rubbers, J. Membr. Sci., 276 (2006) 145-161.
[33] S.C. Ligon, B. Husár, H. Wutzel, R. Holman, R. Liska, Strategies to reduce oxygen inhibition in photoinduced polymerization, Chem. Rev., 114 (2013) 557-589.
[34] L. Kwisnek, S. Heinz, J.S. Wiggins, S. Nazarenko, Multifunctional thiols as additives in UV-cured PEG-diacrylate membranes for CO_2 separation, J. Membr. Sci., 369 (2011) 429-436.
[35] L. Kwisnek, J. Goetz, K.P. Meyers, S.R. Heinz, J.S. Wiggins, S. Nazarenko, PEG containing thiol–ene network membranes for CO_2 separation: effect of cross-linking on thermal, mechanical, and gas transport properties, Macromolecules, 47 (2014) 3243-3253.

[36] L. Shao, S. Quan, X.-Q. Cheng, X.-J. Chang, H.-G. Sun, R.-G. Wang, Developing cross-linked poly(ethylene oxide) membrane by the novel reaction system for H_2 purification, Int. J. Hydrogen Energy, 38 (2013) 5122-5132.
[37] S. Quan, S. Li, Z. Wang, X. Yan, Z. Guo, L. Shao, A bio-inspired CO_2-philic network membrane for enhanced sustainable gas separation, J. Mater. Chem. A, 3 (2015) 13758-13766.
[38] Z. Dai, L. Ansaloni, D.L. Gin, R.D. Noble, L. Deng, Facile fabrication of CO_2 separation membranes by cross-linking of poly (ethylene glycol) diglycidyl ether with a diamine and a polyamine-based ionic liquid, J. Membr. Sci., 523 (2017) 551-560.
[39] A. Genest, D. Portinha, E. Fleury, F. Ganachaud, The aza-Michael reaction as an alternative strategy to generate advanced silicon-based (macro) molecules and materials, Prog. Polym. Sci., 72 (2017) 61-110.
[40] W. Cheng, D. Wu, Y. Liu, Michael addition polymerization of trifunctional amine and acrylic monomer: a versatile platform for development of biomaterials, Biomacromolecules, 17 (2016) 3115-3126.
[41] C.-Y. Liu, C.-J. Huang, Functionalization of polydopamine via the aza-Michael reaction for antimicrobial interfaces, Langmuir, 32 (2016) 5019-5028.
[42] G. González, X. Fernández-Francos, À. Serra, M. Sangermano, X. Ramis, Environmentally-friendly processing of thermosets by two-stage sequential aza-Michael addition and free-radical polymerization of amine–acrylate mixtures, Polym. Chem., 6 (2015) 6987-6997.
[43] J. Wang, H. He, R.C. Cooper, H. Yang, In situ-forming polyamidoamine dendrimer hydrogels with tunable properties prepared via aza-Michael addition reaction, ACS Appl. Mater. Interfaces, 9 (2017) 10494-10503.
[44] O. Konuray, X. Fernández-Francos, X. Ramis, À. Serra, State of the art in dual-curing acrylate systems, Polymers, 10 (2018) 178.
[45] A.O. Konuray, X. Fernández-Francos, À. Serra, X. Ramis, Sequential curing of amine-acrylate-methacrylate mixtures based on selective aza-Michael addition followed by radical photopolymerization, Eur. Polym. J., 84 (2016) 256-267.
[46] J. Wang, G.S. Williamson, I. Lancina, G. Michael, H. Yang, Mildly cross-linked dendrimer hdrogel prepared via aza-Michael adition reaction for tpical bimonidine dlivery, J. Biomed. Nanotechnol., 13 (2017) 1089-1096.
[47] D. Fournier, R. Hoogenboom, U.S. Schubert, Clicking polymers: a straightforward approach to novel macromolecular architectures, Chem. Soc. Rev., 36 (2007) 1369-1380.
[48] S. Luo, Q. Zhang, T.K. Bear, T.E. Curtis, R.K. Roeder, C.M. Doherty, A.J. Hill, R. Guo, Triptycene-containing poly(benzoxazole-co-imide) membranes with enhanced mechanical strength for high-performance gas separation, J. Membr. Sci., 551 (2018) 305-314.
[49] L. Deng, M.-B. Hägg, Swelling behavior and gas permeation performance of PVAm/PVA blend FSC membrane, J. Membr. Sci., 363 (2010) 295-301.
[50] S. Zhao, Z. Wang, Z. Qiao, X. Wei, C. Zhang, J. Wang, S. Wang, Gas separation membrane with CO_2-facilitated transport highway constructed from amino carrier containing nanorods and macromolecules, J. Mater. Chem. A, 1 (2013) 246-249.
[51] Y. Zhao, W.W. Ho, Steric hindrance effect on amine demonstrated in solid polymer membranes for CO_2 transport, J. Membr. Sci., 415 (2012) 132-138.
[52] M. Saeed, S. Rafiq, L.H. Bergersen, L. Deng, Tailoring of water swollen PVA membrane for hosting carriers in CO_2 facilitated transport membranes, Sep. Purif. Technol., 179 (2017) 550-560.
[53] L. Deng, M.-B. Hägg, Fabrication and evaluation of a blend facilitated transport membrane for CO_2/CH_4 separation, Ind. Eng. Chem. Res., 54 (2015) 11139-11150.

[54] S. Kasahara, E. Kamio, T. Ishigami, H. Matsuyama, Effect of water in ionic liquids on CO_2 permeability in amino acid ionic liquid-based facilitated transport membranes, J. Membr. Sci., 415 (2012) 168-175.
[55] Z. Dai, L. Ansaloni, J.J. Ryan, R.J. Spontak, L. Deng, Nafion/IL hybrid membranes with tuned nanostructure for enhanced CO_2 separation: effects of ionic liquid and water vapor, Green Chem., 20 (2018) 1391-1404.
[56] Z. Dai, L. Bai, K.N. Hval, X. Zhang, S. Zhang, L. Deng, Pebax®/TSIL blend thin film composite membranes for CO_2 separation, Sci. China. Chem., 59 (2016) 538-546.
[57] H.Z. Chen, P. Li, T.-S. Chung, PVDF/ionic liquid polymer blends with superior separation performance for removing CO_2 from hydrogen and flue gas, Int. J. Hydrogen Energy, 37 (2012) 11796-11804.
[58] T. Sakaguchi, F. Katsura, A. Iwase, T. Hashimoto, CO_2-permselective membranes of crosslinked poly(vinyl ether)s bearing oxyethylene chains, Polymer, 55 (2014) 1459-1466.
[59] V.A. Kusuma, G. Gunawan, Z.P. Smith, B.D. Freeman, Gas permeability of cross-linked poly(ethylene-oxide) based on poly(ethylene glycol) dimethacrylate and a miscible siloxane co-monomer, Polymer, 51 (2010) 5734-5743.